Article Title:

Unipolar polysaccharide-mediated attachment of the N_2O-reducing bacterium *Bradyrhizobium ottawaense* SG09 to plant roots.

Topic(s) of the paper:

Microbial interactions and signaling with animals and plants

Running headline: *B. ottawaense* utilizes UPP to attach to plants

Authors:

Yudai Takeguchi[1], Ryota Shibuya[2], Momoi Kondo[2], Eriko Betsuyaku[2], Manabu Itakura[3], Kiwamu Minamisawa[3], Masayuki Sugawara[4*], and Shigeyuki Betsuyaku[2*]

Author affiliations:

[1] Graduate School of Agriculture, Ryukoku University, 1-5 Yokotani, Seta Oe-cho, Otsu, Shiga, 520-2194, Japan

[2] Faculty of Agriculture, Ryukoku University, 1-5 Yokotani, Seta Oe-cho, Otsu, Shiga, 520-2194, Japan

[3] Graduate School of Life Sciences, Tohoku University, 2-1-1 Katahira, Aoba-ku, Sendai, Miyagi, 980-8577, Japan

[4] Department of Life and Food Sciences, Obihiro University of Agriculture and Veterinary Medicine, West 2-11, Inada, Obihiro, Hokkaido 080–8555, Japan

[*]Corresponding authors' contact information

Shigeyuki Betsuyaku

E-mail: betsu@agr.ryukoku.ac.jp

Tel: +81-(0)77-599-5655

Masayuki Sugawara

E-mail: msugawara@obihiro.ac.jp

Tel: +81-(0) 155-49-5611

ABSTRACT

Agricultural soils are an important source of nitrous oxide (N_2O), which has greenhouse and ozone-depleting effects. *Bradyrhizobium ottawaense* SG09 is a nitrogen-fixing rhizobium with high N_2O-reducing activity. Rhizobia form symbiotic nodules in leguminous plants. The initial physical attachment of bacteria to plant roots is a critical step in the establishment of symbiotic interactions. In this study, we performed microscopic analysis using DsRed-expressing *B. ottawaense* SG09. We revealed that *B. ottawaense* SG09 attached to both the root surface and root hairs via single cellular poles. This polar attachment was observed not only to the symbiotic host soybean, but also to non-leguminous plants, such as *Arabidopsis*, rice, corn, and wheat. We identified and analyzed the *unipolar polysaccharide* (*upp*) gene cluster, which is proposed to be involved in polar attachment of rhizobia, in the genome of *B. ottawaense* SG09. We established an *Arabidopsis*-based interaction assay and demonstrated that *uppC* and *uppE* play a critical role in attachment to both the root surface and root hairs.

KEYWORDS

Bradyrhizobium ottawaense, N_2O reduction, attachment, adhesin, unipolar polysaccharide

INTRODUCTION

Nitrous oxide (N_2O) is a long-lived greenhouse gas and ozone-depleting substance (Prather et al., 2015). It is released from natural and anthropogenic sources, with more than half of the latter originating from agricultural soils (Tian et al., 2020). *Bradyrhizobium ottawaense* SG09 is a nitrogen-fixing rhizobacterium with high N_2O-reducing activity due to its high expression level of the *nosZ* gene, which encodes nitrous oxide reductase (Wasai-Hara et al., 2020, Wasai-Hara et al., 2023). The application of this bacterium is expected to effectively mitigate agricultural N_2O emissions. However, attempts to infect legumes with specific rhizobial strains in agricultural fields often fail. This problem, which is due to competition between inoculants and indigenous rhizobia, highlights the importance of revealing the molecular basis of legume-rhizobia interactions (Thies et al., 1991).

To establish beneficial symbiosis with legumes, rhizobia form symbiotic structures called nodules where they fix nitrogen. This nodulation process is well studied in *Medicago truncatula* and *Lotus japonicus*. Specifically, flavonoid compounds secreted by plant roots activate the rhizobial NodD transcriptional activator, which induces production of Nod factors (Grundy et al., 2023). When host plant cells perceive Nod factors, infection threads form in root hairs, rhizobia enter these threads, and nodulation occurs (Gage.

71 2004). Prior to all these processes, the attachment of rhizobia to the host root surface is
72 an important initial step. One of the most pronounced features of this process is the
73 attachment of rhizobia to the cell surface of host roots via single cellular poles, as
74 exemplified by several studies in *Agrobacterium tumefaciens* (Matthysse, 2014). Bacteria
75 utilize various adhesive molecules to attach to surfaces (Knights et al., 2021). Among
76 them, the polar adhesin unipolar polysaccharide (UPP), which is widely conserved in
77 *Alphaproteobacteria*, is necessary for polar adhesion to both biotic and abiotic surfaces
78 (Tomlinson and Fuqua 2008, Li et al., 2012, Fritts et al., 2017). Components of the UPP
79 biosynthesis pathway are separately encoded by the core *upp* gene cluster, called
80 *uppABCDEF*, and the others in the other part of the genomes. A similar structure called
81 holdfast, which is conserved in *Caulobacterales*, is well studied in *Caulobacter*
82 *crescentus* (Berne et al., 2015). Production of holdfast requires proteins encoded by the
83 *hfs* gene cluster, called *hfsEFGHCBAD* (Smith et al., 2003, Toh et al., 2008). These two
84 adhesins, UPP and holdfast, are distinct but share some similarities. For example, *uppC*
85 and *uppD* show high sequence similarity to *hfsD* and *hfsE*, respectively (Fritts et al., 2017).
86 Conservation of the *upp* gene cluster in plant-associated *Alphaproteobacteria* such as *A.*
87 *tumefaciens* and *Bradyrhizobium japonicum* suggests that UPP is important for plant-
88 microbe interactions (Xu et al., 2012, Xu et al., 2013, Fritts et al., 2017).
89
90 Several studies have demonstrated that UPP is required for unipolar binding of rhizobia
91 to plant lectins *in vitro*. The plant symbiont *Rhizobium leguminosarum* is reported to
92 utilize a UPP-type adhesin composed of glucomannan for attachment to pea and vetch
93 roots, and this function is required for competitive nodule infection of pea roots (Laus et
94 al., 2006; Williams et al., 2008, Knights et al., 2021). However, the role of the core *upp*

95 gene cluster in *B. ottawaense* SG09 in the association with plants remains to be elucidated.
96 In this study, we investigated the initial attachment of *B. ottawaense* SG09 to plant roots.
97 We successfully visualized *B. ottawaense* SG09 using DsRed and revealed that this
98 bacterium attached to the surface of root epidermal cells including root hairs via single
99 cellular poles. This polar adhesion was observed not only in the interaction with the
100 symbiotic host plant soybean, but also with non-leguminous plants, such as *Arabidopsis*,
101 rice, corn, and wheat. We identified genes encoding the core *upp* gene cluster in the *B.*
102 *ottawaense* SG09 genome and quantitatively evaluated their roles in the initial attachment
103 to plant roots using deletion mutants of *uppC* and *uppE*.
104

105 **MATERIALS AND METHODS**

106 **Bacterial strains and growth conditions**

107 *B. ottawaense* strains were grown aerobically at 30°C in HM salt medium (Cole and Elkan,
108 1973) supplemented with 0.1% arabinose and 0.025% (w/v) yeast extract. *Escherichia*
109 *coli* strains were grown at 37°C in Luria–Bertani medium. The following antibiotics were
110 added appropriately: 300 mg L^{-1} neomycin (Nm) or 50 mg L^{-1} polymyxin B (Px) for *B.*
111 *ottawaense* SG09 and 50 mg L^{-1} kanamycin for *E. coli*.

112

113 DsRed-expressing *B. ottawaense* SG09 (SG09-DsRed) was generated using the pUT-
114 based mini-Tn5 vector pBjGroEL4::DsRed2 carrying the DsRed2 sequence under the
115 control of the BjGroEL4 constitutive promoter (Hayashi et al., 2014). All SG09-DsRed
116 strains were grown in TY medium (5 g/L tryptone, 3 g/L yeast extract, and 1.3 g/L $CaCl_2 \cdot$
117 $2H_2O$) containing 100 μg/mL spectinomycin at 28°C for 4–7 days.

118

119 **Construction of *uppE* and *uppC* deletion mutants**

120 A mobilizable plasmid for generating the in-frame *uppE* deletion mutant (SG09DΔ*uppE*)
121 was constructed as follows: a 0.9-kb fragment containing the 5' flanking region of *uppE*
122 (SG09_60820) and a fragment containing its 3′ flanking region were amplified by PCR
123 from genomic DNA of *B. ottawaense* SG09 using the primer sets
124 uppE_mutF1/uppE_mutR1 and uppE_mutF2/uppE_mutR2, respectively. The two PCR
125 products were fused by overlap extension PCR, and the fused fragment was cloned into
126 the *Sma*I site of pK18*mobsacB* (Schäfer et al., 1994) using an In-Fusion® HD Cloning
127 Kit (Takara Bio Inc., Kusatsu, Japan). The resulting plasmid (pMS195) was transferred
128 from *E. coli* S17-1λpir to SG09-DsRed by biparental mating. An Nm/Px-resistant and
129 sucrose-sensitive transconjugant was selected for single-crossover insertion of the
130 plasmid into the chromosome. Cells were grown in HM liquid medium and spread on HM
131 agar medium containing Px and 10% (w/v) sucrose to rescreen for sucrose-resistant
132 colonies. The selected clones were further screened for Nm sensitivity. Double-crossover
133 events and an in-frame deletion of *uppE* were confirmed by PCR using the primers
134 uppE_F3/uppE_R3, and the nucleotide sequence of *uppE* in the mutants was determined
135 by Eurofins Genomics (Tokyo, Japan) based on the Sanger method.

136

137 To generate the in-frame *uppC* deletion mutant (SG09DΔ*uppC*), a mobilizable plasmid
138 was constructed as follows: a 0.7-kb fragment containing the 5' flanking region of *uppC*
139 (SG09_08120) and a fragment containing its 3′ flanking region were amplified by PCR
140 from genomic DNA of *B. ottawaense* SG09 using the primer sets
141 uppC_mutF1/uppC_mutR1 and uppC_mutF2/uppC_mutR2, respectively. The two PCR

142 products were fused by overlap extension PCR, and the fused fragment was cloned into
143 the *Sma*I site of pK18*mobsacB* as described above. The resulting plasmid (pMS196) was
144 transferred from *E. coli* S17-1λpir to SG09-DsRed by biparental mating. The double-
145 crossover mutants were selected as described above and confirmed by PCR using the
146 primers uppC_F3/uppC_R3 and Sanger sequencing. The oligonucleotide primers used in
147 this study are listed in Table S1.
148
149 **Plant growth conditions**
150 Seeds of *Glycine max* cv. Enrei, *Arabidopsis thaliana* ecotype Col-0, *Oryza sativa* cv.
151 Nipponbare, *Triticum aestivum* cv. Satonosora, and sweet corn (*Zea mays*) Wakuwaku
152 Corn 82 Hybrid (Kaneko Seeds, Gunma, Japan) were used for microscopic analysis.
153 Sterilized *Arabidopsis* seeds were plated and grown on 1/2 MS media (M0404; Sigma-
154 Aldrich, St. Louis, Missouri, USA) containing 0.3% phytagel (P8169; Sigma-Aldrich, St.
155 Louis, Missouri, USA) at 23°C with 24 h of light for the indicated number of days. The
156 other seeds were sterilized and grown on 1.5% agar plates at 25°C for the indicated
157 number of days.
158
159 **Confocal microscopy of bacterial interactions with various plant roots**
160 Three- to five-day-old seedings were inoculated. Bacterial cells grown on TY media were
161 resuspended in sterile water and adjusted to an optical density at 600 nm (OD_{600}) of 0.003
162 for inoculation of soybean (4-day-old), rice (4-day-old), *Arabidopsis* (5-day-old), and
163 wheat (3-day-old) and an OD_{600} of 0.03 for inoculation of sweet corn (3-day-old). The
164 seedlings were incubated with 3 mL of the bacterial suspension at the indicated
165 concentrations in 35-mm cell culture dishes with tissue culture-treated surfaces (3000-

166 035; IWAKI, Shizuoka, Japan). The roots of overnight-treated seedlings were excised,
167 washed once with sterile water, and mounted between the glass surface of a glass-bottom
168 dish (3910-035, IWAKI) and a 1/2 MS phytagel block. Fluorescence confocal and
169 reflection imaging were performed using an LSM980 Airyscan 2 confocal microscope
170 equipped with an LD LCI Plan-Apochromat 40×/1.2 Imm Corr DIC M27 objective and
171 ZEN software (Carl Zeiss Microscopy, Oberkochen, Germany).
172

173 **Quantification of bacterial attachment to the root surface**

174 Five-day-old Col-0 seedings were inoculated. Bacterial cells were prepared as described
175 above. Six seedlings were submerged in 10 mL of the bacterial suspension (OD_{600}=0.003)
176 in an Aznol Petri Dish JP, φ90×15 mm (AS ONE, Osaka Japan) and incubated in this
177 suspension at 23°C for 24 h in the dark. Prior to microscopic analysis, seedlings were
178 washed twice with sterile water. The root surface area located 5 mm from the first root
179 hair that appeared from the shoot side was selected for image acquisition using a BX53
180 fluorescence microscope equipped with a UPLFLN 40× objective and cellSens Standard
181 software (Evident, Tokyo Japan) (Fig. S1). A circle with a radius of 50 μm centered on
182 the root in the microscopic image was selected as the count area, but lateral roots and
183 lateral root primordia were excluded, using Fiji (a distribution of ImageJ, version
184 2.14.0/1.54p) (Fig. S1A). Experiments were performed with six biological replicates and
185 repeated three times individually.
186

187 **Quantification of bacterial attachment to root hairs**

188 Four-day-old Col-0 seedings were inoculated. Bacterial inoculation was performed as
189 described above. After inoculation, the seedlings were incubated at 23°C for 3 h in the

190 dark. Prior to microscopic analysis, plants were washed twice with sterile water. An area
191 of the root centered 2.5 mm from the first root hair from the root tip side was selected for
192 image acquisition using a BX53 fluorescence microscope equipped with a UPLFLN 10×
193 objective and cellSens Standard software (Evident) (Fig. S1B). A square measuring 1 × 1
194 mm^2 centered on the root within the microscopic images was selected for counting using
195 Fiji (a distribution of ImageJ, version 2.14.0/1.54g) (Fig. S1B). The number of bacteria
196 per root hair was counted, and root hairs were classified into three groups based on the
197 bacterial count: 0 (class I), 1–5 (class II), and 6 and more (class III). Experiments were
198 performed with 3–6 biological replicates and repeated three times individually.
199

200 **RESULTS**

201 ***B. ottawaense* SG09 exhibits unipolar binding to the root surface**

202 To gain insights into the initial physical interaction between *B. ottawaense* SG09, which
203 has high N_2O-reducing activity, and plant root tissues, we focused on soybean, a potential
204 agricultural target for practical application of this bacterium. Rhizobial attachment to
205 legume roots is affected by environmental factors such as soil pH (Knights et al., 2021).
206 To simplify the comparison, we developed a simple incubation assay using aseptically
207 germinating soybean seedlings together with *B. ottawaense* SG09 carrying
208 chromosomally integrated DsRed2 under the control of a constitutive promoter (SG09-
209 DsRed) in sterile water. Confocal laser scanning microscopy and confocal reflection
210 microscopy (CRM) were employed to visualize DsRed fluorescence from SG09-DsRed
211 cells and non-fluorescently labeled plant tissue structures, respectively, allowing
212 reconstruction of the three-dimensional (3D) structure of bacterial attachment to plant
213 tissues (Paddock, 2002; Kiyokawa et al., 2017). After incubation for 24 h, the roots were

214 washed and analyzed. Confocal laser scanning microscopy and CRM revealed that
215 multiple SG09-DsRed cells adhered to the soybean root epidermal surface via single poles,
216 resembling well-known characteristics of rhizobia (Fig. 1A and Supplementary Movie 1)
217 (Fritts et al., 2017). An orthogonal projection of the reconstituted 3D structure clearly
218 visualized unipolar attachment of individual SG09-DsRed cells to the plant cell surface
219 (Fig. 1B). Next, we examined if this unipolar adhesion to the plant cellular surface is
220 specific to soybean, which *B. ottawaense* SG09 establishes a symbiotic relationship with
221 through nodulation (Wasai-Hara et al., 2020). When similarly incubated with the roots of
222 rice, wheat, sweet corn, and even *Arabidopsis*, SG09-DsRed cells attached to all the roots
223 examined via single cellular poles (Fig. 2, Fig. S2, Supplementary Movies 2 and 3). Such
224 unipolar attachment was not only observed to root epidermal surfaces but also to root
225 hairs (an example of rice root hairs is shown in Fig. 2D and E, Supplementary Movie 4).
226 These results showed that *B. ottawaense* SG09 adhered to the cellular surfaces of various
227 plant species without any specific preference.
228

229 **The core *upp* gene cluster is conserved in the *B. ottawaense* SG09 genome**

230 UPP was previously reported to be required for bacterial polar attachment; therefore, we
231 investigated whether *B. ottawaense* SG09 possesses homologous genes to *uppABCDEF*
232 of *R. palustris* CGA009 (Fritts et al., 2017; Onyeziri, et al., 2022). BLASTP analysis
233 identified homologous genes in the *B. ottawaense* SG09 genome for each of the *R.*
234 *palustris* CGA009 genes, and these homologs were consequently designated *uppA*, *uppB*,
235 *uppC*, *uppD*, *uppE*, and *uppF* in *B. ottawaense* SG09 (Fig. 3A, Table S2). The core *upp*
236 gene cluster in the *B. ottawaense* SG09 genome consists of *uppABDEF*, while *uppC* is
237 located separately, showing synteny with that of *B. japonicum* USDA 110 (Fritts et al.,

238 2017). *uppC* and *uppE* in *R. palustris* and *A. tumefaciens* play a crucial role in production
239 of UPP; therefore, we generated SG09-DsRed in-frame deletion mutants of *uppC* and
240 *uppE*, called SG09DΔ*uppC* and SG09DΔ*uppE* (Fig. 3B and C) (Fritts et al., 2017;
241 Onyeziri, et al., 2022).
242
243 ***uppC* and *uppE* are required for attachment of *B. ottawaense* SG09 to plant surfaces**
244 Functional analysis of bacterial mutants in terms of their polar attachment is often
245 performed using *in vitro* assays such as the biofilm formation and lectin-binding assays.
246 The use of cultured soybean cells and a specific antibody against a *B. japonicum* strain
247 enabled a more direct and quantitative binding assay with plant cells, but it is costly and
248 labor-intensive to raise specific antibodies and maintain cell cultures (Ho et al., 1988).
249 Considering that SG09-DsRed exhibits unipolar attachment to roots of a small plant,
250 *Arabidopsis*, in addition to soybean, we microscopically investigated the roles of *uppC*
251 and *uppE* using *Arabidopsis* ecotype Col-0 as a host in a small-scale, direct, and
252 quantitative attachment assay. We designed two assays to characterize SG09DΔ*uppC* and
253 SG09DΔ*uppE*, along with SG09-DsRed, in terms of epidermal and root hair attachment
254 (see Materials and Methods). Although the number of SG09-DsRed that attached to the
255 root surface varied greatly among root samples, significantly fewer SG09DΔ*uppC* and
256 SG09DΔ*uppE* than SG09-DsRed attached (Fig. 4). Additionally, significantly fewer
257 SG09DΔ*uppC* than SG09DΔ*uppE* attached to the root surface (Fig. 4).
258
259 Next, we focused on root hair attachment. There was great variation in the number of
260 bacteria that attached to root hairs; therefore, root hair attachment was analyzed by
261 classifying the observed phenotypes into three categories based on the number of attached

262 bacterial cells: 0 (class I), 1–5 (class II), and 6 and more (class III). Compared with SG09-
263 DsRed, both mutants exhibited a significant increase in the number of class I root hairs
264 (Fig. 5A) and a significant reduction in the number of class III root hair (Fig. 5C). In
265 terms of the numbers of class I and class III root hairs, SG09DΔ*uppC* had a significantly
266 more severe phenotype than SG09DΔ*uppE* (Fig. 5A and C). The number of class II root
267 hairs did not significantly differ among the tested strains, suggesting that this class reflects
268 accidental attachment of bacterial cells to root hairs (Fig. 5B). Taken together, our
269 quantitative microscopic analysis reveals that UppC and UppE play a direct and essential
270 role in attachment of *B. ottawaense* SG09 cells to the root epidermal surface and root
271 hairs.
272

273 **DISCUSSION**

274 In this study, we demonstrated that *B. ottawaense* SG09 attached to both the root surface
275 and root hairs via single cellular poles. This attachment was observed not only to soybean,
276 a symbiotic leguminous host for this bacterium, but also to non-leguminous host plants,
277 such as *Arabidopsis*, rice, corn, and wheat. We identified that the *upp* gene cluster is
278 conserved in the *B. ottawaense* SG09 genome. Disruption of *uppC* and *uppE* in *B.*
279 *ottawaense* SG09 significantly reduced attachment of this bacterium to both the root
280 surface and root hairs in *Arabidopsis*. Our assay using *Arabidopsis* provides a high-
281 throughput approach *in planta*. In addition, it enables us to use several genetic tools, *e.g.,*
282 various well-known mutants of plant lectins and immune system components, to
283 molecularly elucidate the interactions of *B. ottawaense* SG09 with plants.
284

285 There is a marked phenotypic difference between SG09DΔ*uppC* and SG09DΔ*uppE*,

286 suggesting that UppC plays a crucial role in attachment to both the root surface and root
287 hairs. *uppC* and *uppE* encode the Wza-type outer membrane polysaccharide secretin and
288 WbaP-initiating glycosyltransferase, respectively, in *A. tumefaciens* (Onyeziri et al.,
289 2022). In *A. tumefaciens*, *uppE* is necessary for UPP production under inorganic
290 phosphate-rich conditions, while *uppE* and its paralog *Atu0102* act redundantly under
291 inorganic phosphate-limited conditions (Xu et al., 2012). Thus, other genes might
292 function redundantly with *uppE* in the *B. ottawaense* SG09 genome. Our findings suggest
293 that UPP is important for attachment of *B. ottawaense* SG09 to biotic surfaces. Further
294 information is essential to elucidate the function of UPP in *B. ottawaense* SG09, *e.g.,* the
295 biochemical composition that governs lectin specificity (Onyeziri et al., 2022). However,
296 it is difficult to determine the biochemical composition of UPP because of its insolubility
297 and low level of synthesis by bacterial cells (Berne et al., 2015, Thompson et al., 2018).
298
299 *B. ottawaense* SG09 is gaining attention because of its high N_2O-reducing activity
300 (Wasai-Hara et al., 2023). Further optimization is required to exploit *B. ottawaense* SG09
301 as an N_2O-reducing agent in agricultural fields, including overcoming the competitive
302 effects of indigenous bacteria (Thies et al., 1991, Wasai-Hara et al., 2023). The initial
303 process of bacterial attachment to the root surface could be an important target for
304 inoculated bacteria to successfully dominate during nodulation. In this study, we
305 established a small-scale, direct, and quantitative *in planta* assay using *Arabidopsis* as a
306 host, which could broaden our knowledge of the mechanisms underlying rhizobial
307 attachment. Further research may lead to engineering of rhizobial adhesins that improve
308 the probability of attachment and the development of methods that overcome indigenous
309 bacteria.

Acknowledgements

This work was supported by project JPNP18016, subsidized by the New Energy and Industrial Technology Development Organization (NEDO).

Conflicts of Interest

The authors declare that there are no conflicts of interest.

REFERENCES

Cole, M. A. & Elkan, G. H. Transmissible resistance to penicillin G, neomycin, and chloramphenicol in *Rhizobium japonicum*. *Antimicrob Agents Chemother* **4**, 248-253 (1973).

Berne, C., Ducret, A., Hardy, G. G., & Brun, Y. V. (2015). Adhesins Involved in Attachment to Abiotic Surfaces by Gram-Negative Bacteria. Microbiology spectrum, 3(4), 10.1128.

Fritts, R. K., LaSarre, B., Stoner, A. M., Posto, A. L., & McKinlay, J. B. (2017). A Rhizobiales-Specific Unipolar Polysaccharide Adhesin Contributes to *Rhodopseudomonas palustris* Biofilm Formation across Diverse Photoheterotrophic Conditions. Applied and environmental microbiology, 83(4), e03035-16.

Gage D. J. (2004). Infection and invasion of roots by symbiotic, nitrogen-fixing rhizobia

during nodulation of temperate legumes. Microbiology and molecular biology reviews : MMBR, 68(2), 280–300.

Grundy, E. B., Gresshoff, P. M., Su, H., & Ferguson, B. J. (2023). Legumes Regulate Symbiosis with Rhizobia via Their Innate Immune System. International journal of molecular sciences, 24(3), 2800.

Hayashi, M., Shiro, S., Kanamori, H., Mori-Hosokawa, S., Sasaki-Yamagata, H., Sayama, T., et al. (2014) A Thaumatin-Like Protein, Rj4, Controls Nodule Symbiotic Specificity in Soybean. *Plant Cell Physiol*. 55: 1679–1689.

Ho, S.C., Ye, W.Z., Schindler, M., and Wang, J.L. (1988) Quantitative assay for binding of Bradyrhizobium japonicum to cultured soybean cells. *J Bacteriol*. 170: 3882–3890.

Kiyokawa, T., Usuba, R., Obana, N., Yokokawa, M., Toyofuku, M., Suzuki, H., et al. (2017) A Versatile and Rapidly Deployable Device to Enable Spatiotemporal Observations of the Sessile Microbes and Environmental Surfaces. *Microbes Environment*. 32: ME16161.

Knights, H. E., Jorrin, B., Haskett, T. L., & Poole, P. S. (2021). Deciphering bacterial mechanisms of root colonization. Environmental microbiology reports, 13(4), 428–444.

Laus, M. C., Logman, T. J., Lamers, G. E., Van Brussel, A. A., Carlson, R. W., & Kijne, J. W. (2006). A novel polar surface polysaccharide from *Rhizobium leguminosarum* binds

host plant lectin. Molecular microbiology, 59(6), 1704–1713.

Li, G., Brown, P. J., Tang, J. X., Xu, J., Quardokus, E. M., Fuqua, C., & Brun, Y. V. (2012). Surface contact stimulates the just-in-time deployment of bacterial adhesins. Molecular microbiology, 83(1), 41–51.

Onyeziri, M. C., Hardy, G. G., Natarajan, R., Xu, J., Reynolds, I. P., Kim, J., Merritt, P. M., Danhorn, T., Hibbing, M. E., Weisberg, A. J., Chang, J. H., & Fuqua, C. (2022). Dual adhesive unipolar polysaccharides synthesized by overlapping biosynthetic pathways in *Agrobacterium tumefaciens*. Molecular microbiology, 117(5), 1023–1047.

Paddock, S. (2002) Confocal reflection microscopy: the “other” confocal mode. *Biotechniques*. 32: 274, 276–8.

Prather, M. J., Hsu, J., DeLuca, N. M., Jackman, C. H., Oman, L. D., Douglass, A. R., Fleming, E. L., Strahan, S. E., Steenrod, S. D., Søvde, O. A., Isaksen, I. S., Froidevaux, L., & Funke, B. (2015). Measuring and modeling the lifetime of nitrous oxide including its variability. Journal of geophysical research. Atmospheres : JGR, 120(11), 5693–5705.

Schäfer, A. *et al.* Small mobilizable multi-purpose cloning vectors derived from the *Escherichia coli* plasmids pK18 and pK19: selection of defined deletions in the chromosome of *Corynebacterium glutamicum*. *Gene* **145**, 69-73 (1994).

Smith, C. S., Hinz, A., Bodenmiller, D., Larson, D. E., & Brun, Y. V. (2003). Identification of genes required for synthesis of the adhesive holdfast in *Caulobacter crescentus*. Journal of bacteriology, 185(4), 1432–1442.

Thies, J. E., Singleton, P. W., & Bohlool, B. B. (1991). Influence of the size of indigenous rhizobial populations on establishment and symbiotic performance of introduced rhizobia on field-grown legumes. Applied and environmental microbiology, 57(1), 19–28.

Tian, H., Xu, R., Canadell, J. G., Thompson, R. L., Winiwarter, W., Suntharalingam, P., Davidson, E. A., Ciais, P., Jackson, R. B., Janssens-Maenhout, G., Prather, M. J., Regnier, P., Pan, N., Pan, S., Peters, G. P., Shi, H., Tubiello, F. N., Zaehle, S., Zhou, F., Arneth, A., … Yao, Y. (2020). A comprehensive quantification of global nitrous oxide sources and sinks. Nature, 586(7828), 248–256.

Toh, E., Kurtz, H. D., Jr, & Brun, Y. V. (2008). Characterization of the *Caulobacter crescentus* holdfast polysaccharide biosynthesis pathway reveals significant redundancy in the initiating glycosyltransferase and polymerase steps. Journal of bacteriology, 190(21), 7219–7231.

Tomlinson, A. D., & Fuqua, C. (2009). Mechanisms and regulation of polar surface attachment in *Agrobacterium tumefaciens*. Current opinion in microbiology, 12(6), 708–714.

Thompson, M. A., Onyeziri, M. C., & Fuqua, C. (2018). Function and Regulation of

Agrobacterium tumefaciens Cell Surface Structures that Promote Attachment. Current topics in microbiology and immunology, 418, 143–184.

Wasai-Hara, S., Hara, S., Morikawa, T., Sugawara, M., Takami, H., Yoneda, J., Tokunaga, T., & Minamisawa, K. (2020). Diversity of *Bradyrhizobium* in Non-Leguminous Sorghum Plants: *B. ottawaense* Isolates Unique in Genes for N2O Reductase and Lack of the Type VI Secretion System. Microbes and environments, 35(1), ME19102.

Wasai-Hara, S., Itakura, M., Fernandes Siqueira, A., Takemoto, D., Sugawara, M., Mitsui, H., Sato, S., Inagaki, N., Yamazaki, T., Imaizumi-Anraku, H., Shimoda, Y., & Minamisawa, K. (2023). *Bradyrhizobium ottawaense* efficiently reduces nitrous oxide through high *nosZ* gene expression. Scientific reports, 13(1), 18862.

Williams, A., Wilkinson, A., Krehenbrink, M., Russo, D. M., Zorreguieta, A., & Downie, J. A. (2008). Glucomannan-mediated attachment of *Rhizobium leguminosarum* to pea root hairs is required for competitive nodule infection. Journal of bacteriology, 190(13), 4706–4715.

Xu, J., Kim, J., Danhorn, T., Merritt, P. M., & Fuqua, C. (2012). Phosphorus limitation increases attachment in *Agrobacterium tumefaciens* and reveals a conditional functional redundancy in adhesin biosynthesis. Research in microbiology, 163(9-10), 674–684.

Xu, J., Kim, J., Koestler, B.J., Choi, J., Waters, C.M., and Fuqua, C. (2013) Genetic analysis of Agrobacterium tumefaciens unipolar polysaccharide production reveals

complex integrated control of the motile-to-sessile switch. *Mol Microbiol*. 89: 929–948.

Figure Legends

Fig. 1. Confocal fluorescence imaging of the roots of soybean seedlings incubated with SG09-DsRed.

(A) Representative reconstituted 3D images of SG09-DsRed (red) binding to soybean roots visualized by CRM (gray). A merged image (left) and the corresponding DsRed image (right) are shown. (B) Orthogonal projection images of the reconstituted 3D image in (A) represented by maximal projection. A merged image (left) and the corresponding DsRed image (right) are shown. Scale bar, 10 μm.

Fig. 2. Confocal fluorescence imaging of the roots of rice and *Arabidopsis* seedlings incubated with SG09-DsRed.

(A) A representative reconstituted 3D image of SG09-DsRed (red) binding to rice roots visualized by CRM (gray). (B) An orthogonal projection image of the reconstituted 3D image in (A) represented by maximal projection. (C) A representative reconstituted 3D image of SG09-DsRed (red) binding to *Arabidopsis* roots visualized by CRM (gray). (D) An orthogonal projection image of the reconstituted 3D image in (C) represented by maximal projection. (E) Representative reconstituted 3D images of SG09-DsRed (red) binding to rice root hairs visualized by CRM (gray). (F)A DsRed image of the 3D images shown in (E). Scale bars, 10 μm.

Fig. 3. The core *upp* gene cluster in the *B. ottawaense* SG09 genome and the mutants

452 generated in this study.

453 (A) Schematic representations of the *upp* gene cluster in the genomes of wild-type *B.*
454 *ottawaense* SG09 and the respective mutants. (B, C) PCR validation of SG09DΔ*uppC*
455 and SG09DΔ*uppE* loci using the primer pairs uppC_F3/uppC_R3 for *uppC* (B) and
456 uppE_F3/uppE_R3 for *uppE* (C). PCR products were separated on 2% agarose gels.

457

458 Fig. 4. Quantification of bacterial attachment to the root surface.

459 Five-day-old Col-0 seedlings were incubated with bacterial suspensions (OD_{600}=0.003).
460 After incubation for 24 h at 23°C in the dark, plants were washed twice with sterile water.
461 The number of epidermally attached bacterial cells present within a circle with a radius
462 of 50 μm set 5 mm away from the first root hair observed from the shoot side was counted.
463 n=10 for SG09-DsRed, n=13 for SG09DΔ*uppC*, and n=15 for SG09DΔ*uppE*. *$p < 0.05$.
464 Statistical analysis was performed by the *t*-test using R (version 4.4.2).

465

466 Fig. 5. Quantification of bacterial attachment to root hairs.

467 Four-day-old Col-0 seedlings were incubated with bacterial suspensions (OD_{600}=0.3).
468 After incubation for 3 h at 23°C in the dark, plants were washed twice with sterile water.
469 A one mm square centered 2.5 mm from the first root hair from the root tip side was used
470 for bacterial counting. The number of bacterial cells attached to each root hair was
471 counted and then root hairs are classified into three groups based on the number of
472 attached bacteria: 0 (A, class I), 1–5 (B, class II), and 6 and more (C, class III). n=14. *p
473 < 0.05; ns, not significant. Statistical analysis was performed by the *t*-test using R (version
474 4.4.2).

Figure 1.

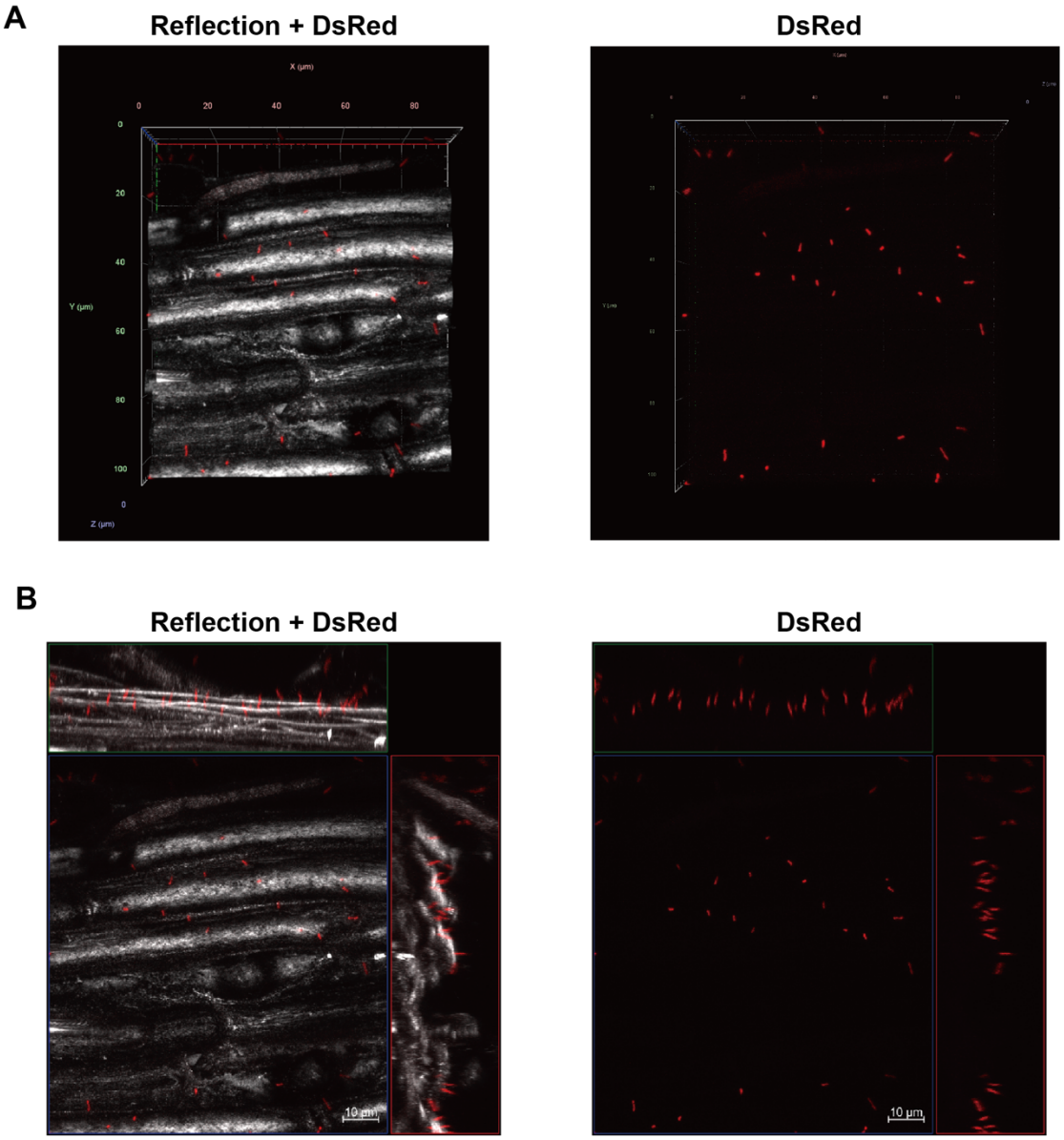

Figure 1.

Figure 2.

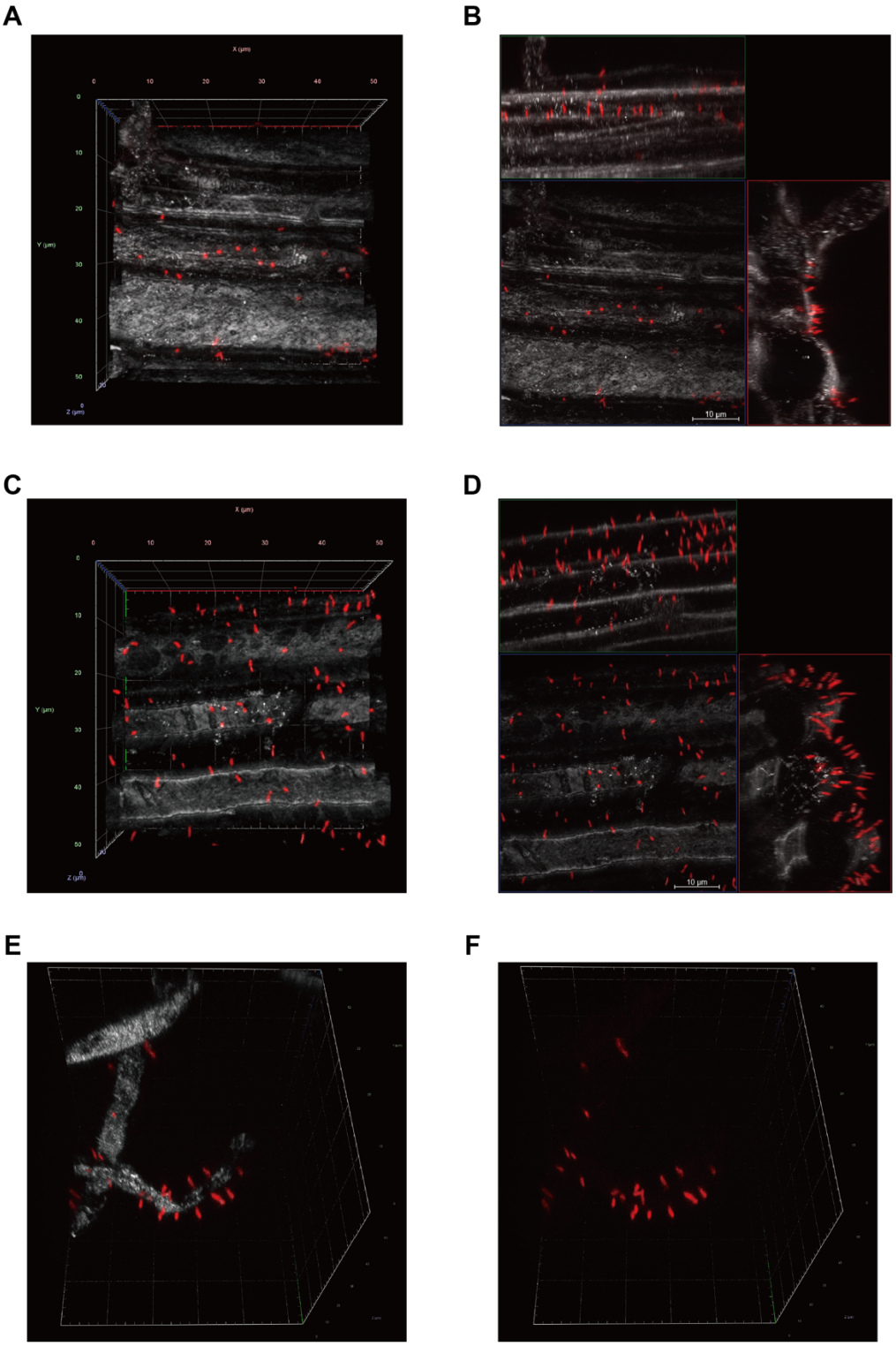

Figure 2.

481

Figure 3.

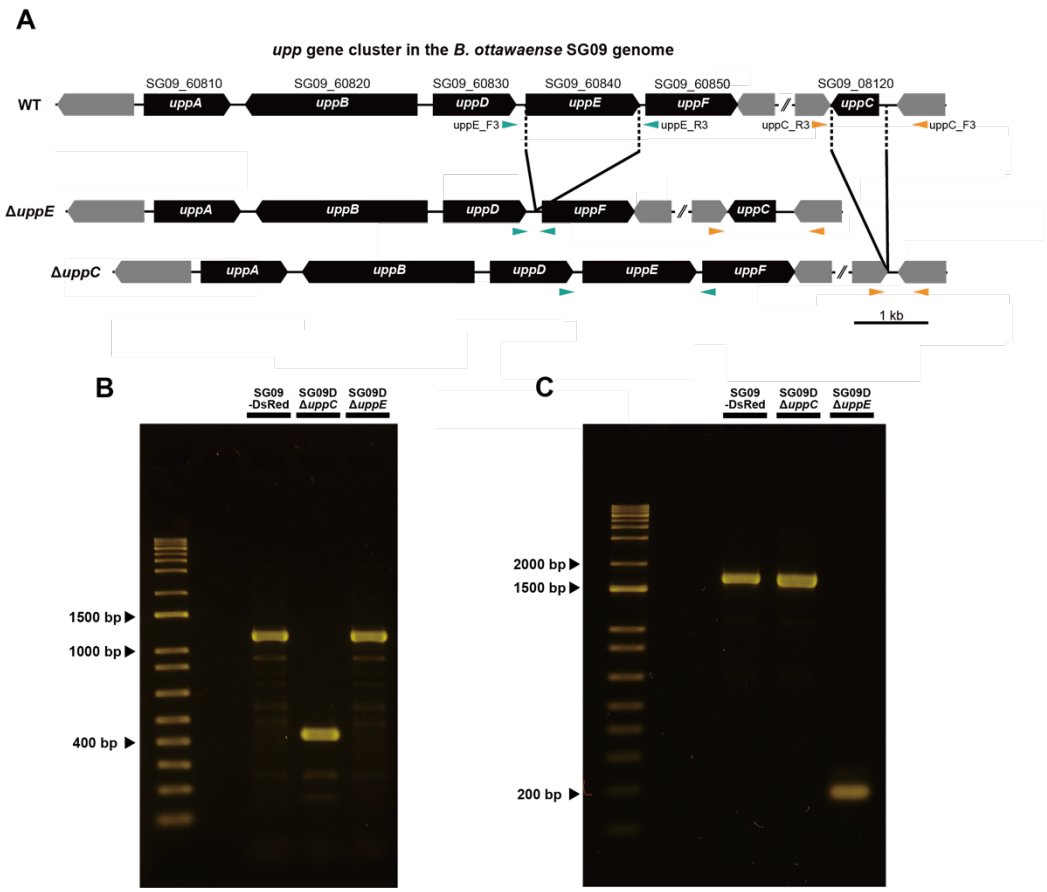

482

483 Figure 3.

Figure 4.

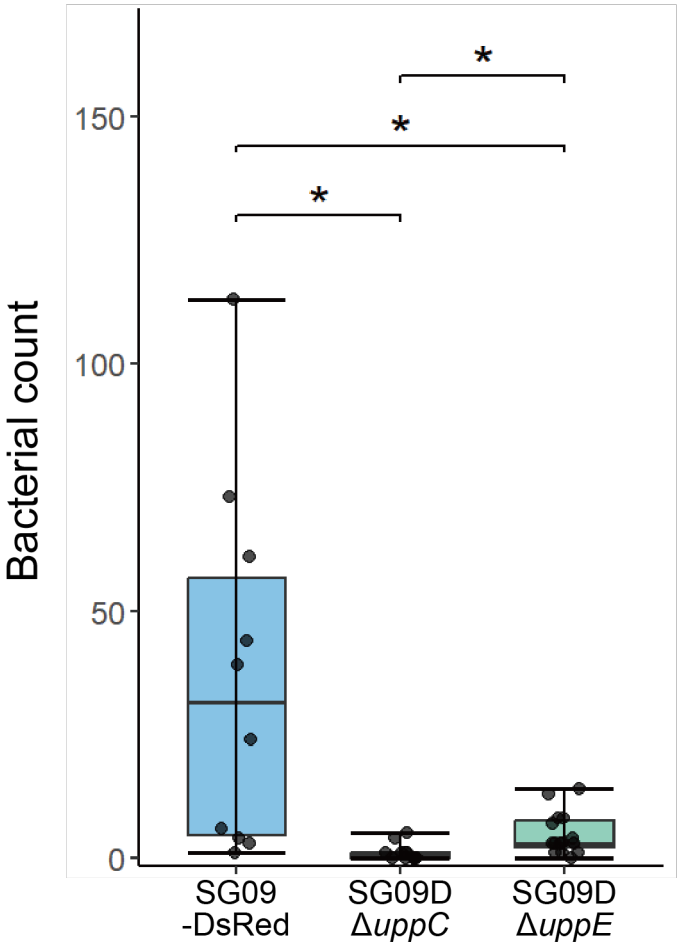

484

485 Figure 4.

Figure 5.

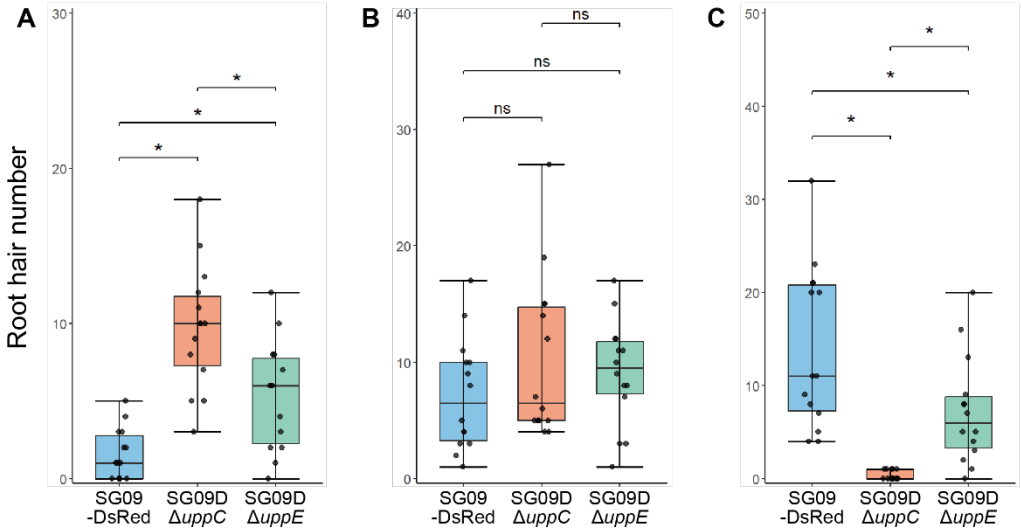

Figure 5.

494 **Supplementary Materials**

495

Figure S1.

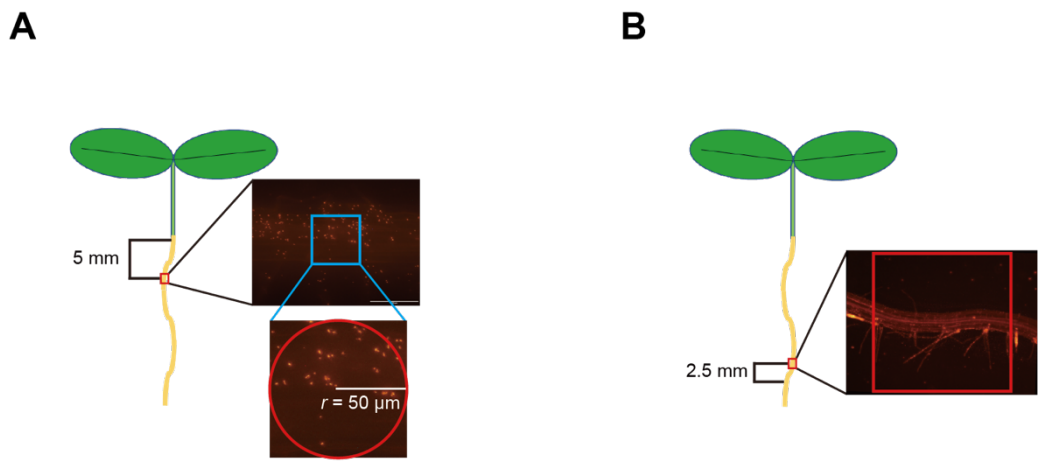

496

497 Figure S1. Schematic diagrams showing the measurement methods used in this study.

498 (A) Root surface attachment analysis. A circle with a radius of 50 μm centered on the root

499 (shown in red) located 5 mm from the first root hair in the microscopic image was used

500 for bacterial counting. (B) Root hair attachment analysis. The number of bacterial cells

501 per root hair in a one mm square centered on the root (shown in red) located 2.5 mm from

502 the first root hair from the root tip side was used for bacterial counting.

Figure S2.

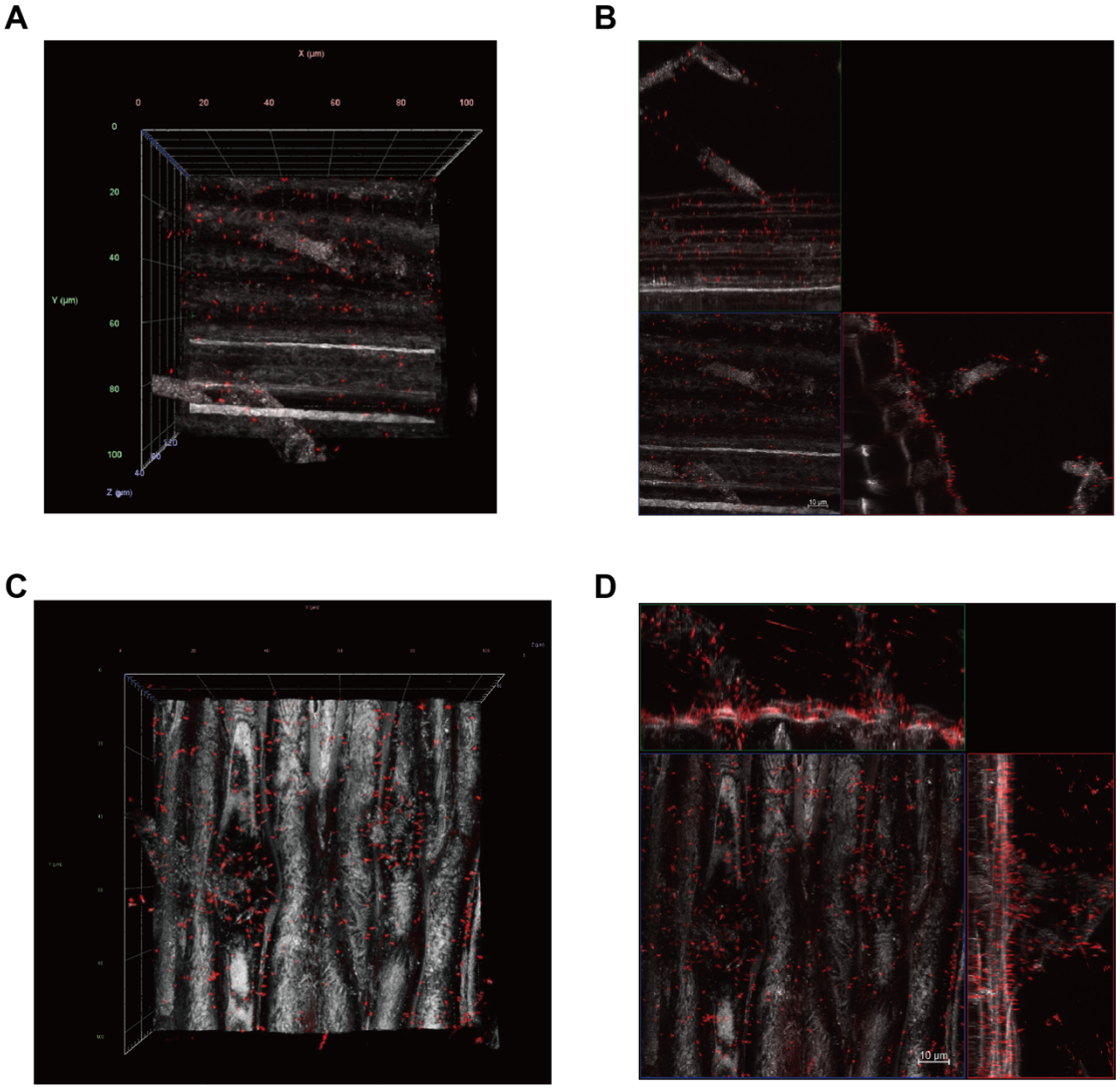

Figure S2. Confocal fluorescence imaging of the roots of wheat and sweet corn seedlings incubated with SG09-DsRed.

506 (A) A representative reconstituted 3D image of SG09-DsRed (red) binding to wheat roots
507 visualized by CRM (gray). (B) An orthogonal projection image of the reconstituted 3D
508 image in (A) represented by maximal projection. (C) A representative reconstituted 3D
509 image of SG09-DsRed (red) binding to sweet corn roots visualized by CRM (gray). (D)
510 An orthogonal projection image of the reconstituted 3D image in (C) represented by
511 maximal projection. Scale bars, 10 μm.
512
513 Supplementary Movie 1. Reconstituted 3D rendering of SG09-DsRed (red) binding to
514 soybean roots visualized by CRM (gray) shown in Fig. 1A.
515
516 Supplementary Movie 2. Reconstituted 3D rendering of SG09-DsRed (red) binding to
517 rice roots visualized by CRM (gray) shown in Fig. 2A.
518
519 Supplementary Movie 3. Reconstituted 3D rendering of SG09-DsRed (red) binding to
520 *Arabidopsis* roots visualized by CRM (gray) shown in Fig. 2C.
521
522 Supplementary Movie 4. Reconstituted 3D rendering of SG09-DsRed (red) binding to
523 rice root hairs visualized by CRM (gray).
524
525
526
527
528
529

530 Table S1.

Table S1. Primers used in this study

Primer name	Sequence (5' to 3')
uppC_mutF1	TCGAGCTCGGTACCCCGACCACCCATTTCGTCAAC
uppC_mutR1	TGGATTTCAGGCGGTGAGCGAGACGGCTTAAGTGATGC
uppC_mutF2	GCATCACTTAAGCCGTCTCGCTCACCGCCTGAAATCCA
uppC_mutR2	CTCTAGAGGATCCCCTTTGAAATAGGGCGCGTCTC
uppC_F3	CCTATTCCGATGCGCAGAAG
uppC_R3	CATCGACGCTAACAGGATCG
uppE_mutF1	TCGAGCTCGGTACCCCGCTGCATTATCCCCTCAAC
uppE_mutR1	CGGGGCATGACGGAAAACTCCACGTCCATTTCAAGCAC
uppE_mutF2	GTGCTTGAAATGGACGTGGAGTTTTCCGTCATGCCCCG
uppE_mutR2	CTCTAGAGGATCCCCGTGGAATCGAACGACAGCAG
uppE_F3	TAACCATCCTTAAGCCCGCT
uppE_R3	CTATTCGGACGCCAAACACC

531 *The underlined sequences are homologous regions of pK18mobsacB.

532

533 Table S2.

Table S2. BLASTP analysis of the orthologous genes of *uppABCDEF* in *B. ottawaense* SG09

Rhodopseudomonas palustris CGA009	*Bradyrhizobium ottawaense* SG09		
	Locus tag	Position	Identity(%)
RPA2753_UppA	SG09_60810	6502658-6503839	230/390 (59%)
RPA2752_UppB	SG09_60820	6504021-6506357	484/699 (69%)
RPA2751_UppD	SG09_60830	6506563-6507696	262/377 (69%)
RPA2750_UppE	SG09_60840	6507817-6509364	401/519 (77%)
RPA4581_UppF	SG09_60850	6509436-6510692	227/404 (56%)
RPA4833_UppC	SG09_08120	888458-889111	143/217 (66%)

534